# Synthesis of Activated carbon supported AgO and CuO nanocomposites: Characterizations and photo catalytic studies

*T. Sivasankar[1], B. Karthikeyan[1*].*

**[1]Department of Chemistry, Annamalai University, Tamil Nadu, 608 002, India.**

**Abstract**

Synthesized Activated Carbon-supported AgO and CuOnanocomposite are reprted . AC-AgO and AC-CuO nanocomposites are successfully synthesized through a precipitation method. Structural, morphological, and optical characteristics of the composites are evaluated using FT-IR, XRD, FE-SEM, UV-DRS, and PL techniques. The FE-SEM analysis indicates an uniform distribution of the nanocomposites. XRD results demonstrated that the materials exhibit a crystalline structure. The band gap values are measured at 2.68 V for AC-AgO and 1.98V for AC-CuO, indicating that these nanocomposites possess a significant level of semi conductivity. Methylene blue (MB) dye is employed to assess the photocatalytic performance of the composites. The degradation efficiency of the AC-AgO and AC-CuO catalysts are found to be 85.55 and 80.71% for MB dye, respectively. Therefore, the AC-AgO and AC-CuO composite exhibits superior performance against MB dye. A possible mechanism is proposed with highlighting the influence of carbon.

**Keywords:** Activated Carbon, AgO,CuO , Nanocomposite, Degradation , MB dye.

## 1.Introduction

Nanotechnology is a relatively new science with a vast array of applications and unmatched growth. This technique's main method makes use of particles that range in size from 10 to 100 nm. Nanomaterials have applications in biotechnology, medicine, electronics, and medical care, among other fields. Because they are inexpensive, non-toxic, and environmentally friendly, AgNPs hold a significant position among other nanoparticles in the field of technology [1–4].However, the extensive release of hazardous dye waste into aquatic bodies by the textile industry has raised environmental concerns due to its harmful and harmful consequences on both humans and ecosystems. To avoid any potential risks that dyes and their intermediaries may pose, it is imperative that these dyes be mineralized. By creating reactive species by semiconductor illumination, differential photocatalysis has been widely employed to convert dangerous compounds into simpler and safer products [5,6].

These problems can be resolved, though, by developing metal oxide-based nanocomposite architectures. Many titania-based composite nanomaterials, such as $Ag_2O/TiO_2$nanofibers, $Ag@TiO_2$ core shell structures, $TiO_2$/graphene, $TiO_2$/graphene oxide, TiO2-carbon nanotubes (CNTs) composite nanostructures, $TiO_2/g\text{-}C_3N_4$ [6], $TiO_2(B)/Ag_2O$, $ZnO/TiO_2$, graphene-$ZnTiO_3$, reduced graphene oxide (r-GO)/Pd–$TiO_2$/r-GO, and $Ag_2O$/graphene oxide have become promising materials for photocatalysis mediated by visible light and for reducing the rate of electron-hole recombination. Despite their superior photocatalytic efficacy in removing toxic compounds, the physical and chemical procedures used to create these nanocomposites are neither environmentally friendly nor energy-efficient [7]. The synthesis of Ag/ZnO nanocomposites has been reported using a number of methods thus far, including sol-gel, photoreduction, chemical deposition, hydrothermal, and pulsed laser deposition. However, because they call for high pressures, high temperatures, hazardous chemicals, pricey equipment, or lengthy synthesis times, the majority of these methods cannot be used in a commercial setting. To satisfy the demands of the economy and environment, Ag/ZnO nanocomposites require a low-cost, straightforward, and safe method. While a lot of work has been done to create Ag/ZnO nanocomposite, very little of this research has concentrated on green production techniques.

Copper oxides comprise a significant class of transition metal oxides. Cupric oxide (CuO), sometimes referred to as tenorite, is one of the two stable oxides of copper, the other being $Cu_2O$ (cuprous oxide). CuO is a solid that is black. With space group $C_2/c$, CuO displays a monoclinic unit cell in which each Cu atom coordinates with four oxygen atoms. CuO is an important, affordable, and nontoxic p-type semiconductor material with a band gap of 1.2 eV. CuO's physical and chemical properties are of great interest because of its numerous applications in gas sensors, biosensors, photo-detectors, magnetic storage media, supercapacitors, photocatalysis, elimination of inorganic pollutants, and antimicrobial applications [8].

Methylene blue (MB) a cationic dye, is frequently used in the manufacturing of silk clothing. It has harmful properties for many types of life and is believed to be mutagenic and carcinogenic. Additionally, MB-contaminated effluents are produced by the printing, dyeing, rubber, plastic, textile, and paper industries. Because of its solid structure, biodegradation is challenging.So there is a greater need to develop remediation techniques that are successful in eliminating these harmful dye [9-10] Methylene Blue (MB).

## 2. Experimental section

### 2.1 Materials

Silver nitrate ($AgNO_3$), Copper chloride ($CuCl_2.2H_2O$), distilled water, Whatman filter paper, Activated Carbon (Super carbon), 0.8M NaOH, Dye – Methylene blue (MB) were used and henna leaf was collected from annamalainagar.

### 2.2 Henna Leaf extract preparation

Fresh henna leaves were repeatedly cleaned with distilled water to get rid of dirt. The leaves were then left to air dry at room temperature for five days in order to reach the ideal level of dryness. It was then ground into a fine powder using a mortar and pestle. The henna leaf extract was made by mixing 200 mL of distilled water with 10 grams of leaf powder, and it was then heated for 90 minutes at $80^0$C. After letting this solution cool gradually to room temperature, it was filtered using Whatman Grade 1 filter paper and stored in a refrigerator at 5 °C to preserve it for subsequent use.

### 2.2 Synthesis of AC-AgO

After dissolving 0.1M $AgNO_3$ solution in 100 mL of distilled water and magnetically stirring for for 20 minutes at 80°C, 50 mL of henna leaf extract and 100 mL of 0.1M $AgNO_3$ were added, and the precipitate of light black color was produced. Following that, few drops of to 6 mL of 0.8 M NaOH was added to promote the dark black precipitate, which was continually swirled for three hours. Lastly, 0.06 g of Activated carbon was added and mixed continuously for one hour. After filtering, ethanol washing, and three hours of oven drying at 100°C, the sample was stored in a muffle furnace at 550°C for five hours. Dull white AC-AgO NPs was obtained.

### 2.3 Synthesis of AC-CuO

The AC-CuO nanocomposite was created by dissolving a 0.1M $CuCl_2$ solution in 100mL of distilled water, swirling magnetically for 30 minutes at 80°C, and then 50mL of henna leaf extract was added with 100 mL of 0.1M $CuCl_2$ solution. To encourage the dark black precipitate, 0.8 M NaOH was then added in drops, and it was continuously swirled for three hours. Finally, 0.06g of Activated Carbon was added, and for an hour, it was constantly stirred. The sample was held in a muffle furnace at 350°C for three hours following filtering, ethanol washing, and three hours of oven drying at 100°C.

### 2.5 Characterization studies

Cu-Kα radiation (λ = 1.5418 Å) from X-ray system (XPERT PRO) was utilized to analyse the sample diffraction profiles. The material functional groups were assigned by the use of FT-IR (IR Tracer-100 Shimadzu) spectrophotometer. Shimadzu UV-2600 was used to detect diffuse reflectance spectra (UV-vis DRS) between 200 and 800 nm. The sample photoluminescence emission was measured using a Perkin Elmer LS 55 fluorescence spectrometer. Using CARL ZEISS-SIGMA 300 FESEM with the EDAX FE-SEM apparatus model, the morphology of the nanocomposites was examined.

### 2.6 Photocatalytic experiment

For photo degradation of dyes by synthesised nanocompositess, an organic dye Methylene blue was chosen of concentration of $10^{-4}$ M of 100 mL for each photo degradation process with and without catalyst.Using MB dye, the photocatalytic activity of the generated AC-AgO and AC-CuO nanocomposites was examined. The breakdown of MB in 100 mL of clean water was individually photocatalyzed using a 0.0001M dye solution containing 0.1g of the photocatalyst. In the photoreactor chamber, the solution was exposed to UV light 360 nm range, and samples were taken at regular intervals of fifteen minutes. The degradation was evaluated using a UV-visible spectrophotometer, which has a wavelength range of 200 to 800 nm. It was found that 665 nm is the wavelength at which MB dye absorbs.

$$\text{Degradation Rate (\%)} = \frac{C_o - C_t}{C_o} \times 100 \qquad (1)$$

Where, Ct is the concentration of the MB after a certain amount of time, and $C_0$ is the concentration of the MB at the start.

## 3.Results and discussion

### 3.1 FT-IR analysis

FT-IR analysis was performed at room temperature in the range of 400–4000 $cm^{-1}$ (Fig. 1). According to the Fig. 1, the AC-AgO composite metal–oxygen stretching frequencies are reported in the range 480–900 $cm^{-1}$, associated with the vibrations of Ag–O bond. Moreover, bands at 1372 and 1448 $cm^{-1}$ are attributable to the C–O/C–C coupled

stretching [11]. The FT-IR spectrum of CuO shows peaks at 526 and 580 $cm^{-1}$ revealed the formation of CuO as shown in Figure 1 (b). Figure 1(a.b) shows a broad peak noticed at 3430 $cm^{-1}$ attributed to O‑H stretching of the moisture content. O–H bending peak appear at 1620 $cm^{-1}$ due to adsorbed water molecules, and weak bands related to bending vibrations around 1122 $cm^{-1}$. A peak obtained at 2930 $cm^{-1}$ attributed to the C‑H bond [12,13]. Figure 1 (a) shows in FTIR spectra of the nanocomposites, small peaks observed at 2920 and 1372 $cm^{-1}$ indicate the presence of silver nanoparticles.These findings confirm the formation of a stable nanocomposite with synergistic properties from the combination of silver oxide and activated carbon, making it a promising material for applications such as catalysis, photocatalytic activity.

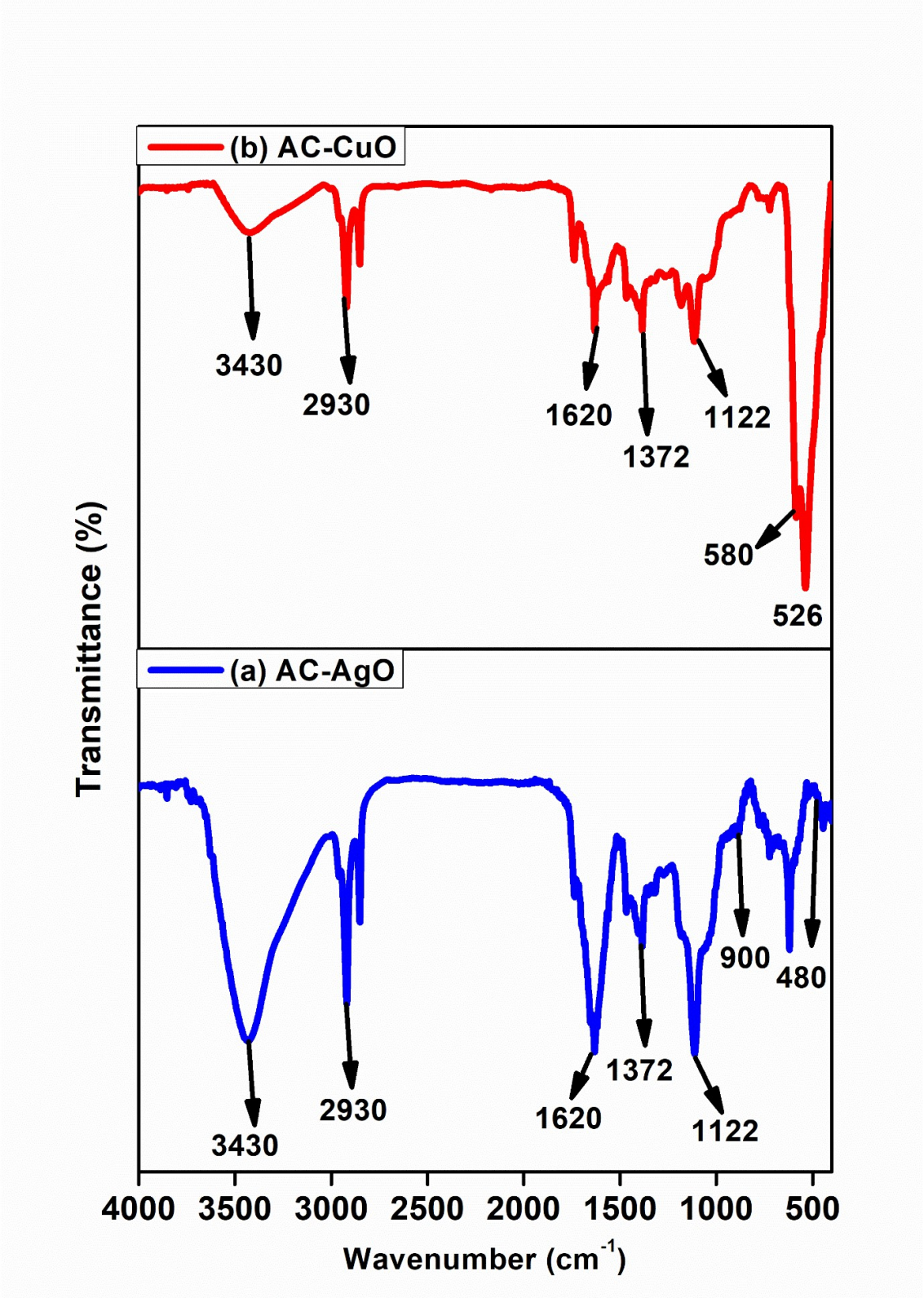


**Figure 1: FT-IR spectrum of (a) AC-AgO and (b) AC-CuO**

### 3.2 XRD analysis

The synthesized AC-AgO and AC-CuO were characterized using the powder X-ray diffraction technique. Figure 2 shows the AC-AgO, AC-CuO XRD pattern. The broadness of the XRD spectrum confirmed that the material is nanocrystalline. The four main distinctive diffraction peaks that were found at 2θ = 38.21 (111), 44.31 (200), 64.49 (220), and 77.29 (311) can be used to identify the cubic phase of Ag. JCPDS.No. 04-0783, it confirms that AgO is present in the sample as shown in Figure 2(a). There were no impurity peaks in the XRD patterns[14].

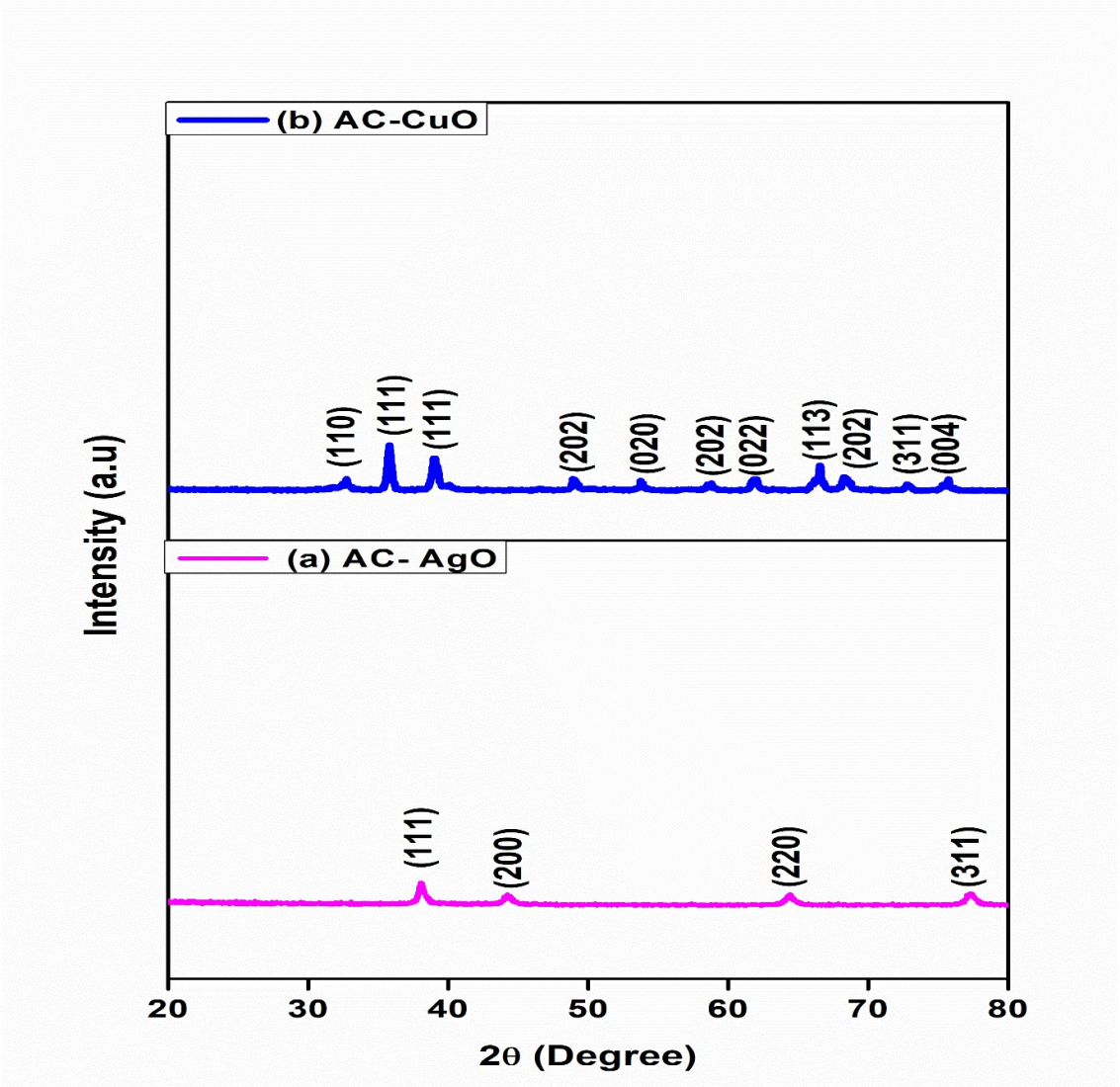


**Figure 2: XRD spectrum of (a) AC-AgO and (b) AC-CuO**

The monoclinic structure of CuO diffraction data (JCPDS card no. 48-1548) is consistent with the well-defined diffraction peak. The XRD patterns showed diffraction peaks (110), (111), (211), (202), (020), (202), (022), (113), (202), (311), and (004) that correspond rather well with the standard diffraction peaks (JCPDS: card no. 48-1548) as shown in figure 2(b) [15]. Figure 2 (a,b) shows based on the detected low-intensity peaks for AC-AgO, the synthetic AC-CuO sample is mainly composed of AgO and CuO nanoparticles (Figure 2). The intensity was reduced if the AC-CuO and AC-CuO was present. Amorphous or disordered carbon is a possibility. A lack of recognizable peaks may arise from this so using below equation to calculate the crystalline size of the sample

$$D = \frac{0.98\lambda}{\beta \mathrm{Cos}\theta} \qquad (2)$$

Where, λ is the X-ray beam operating system wavelength, and θ is the diffraction angle, β is the full-width half maximum determined from the peak of highest intensity, D is the crystalline size. Using equation 2 of the Debye-Scherrer formula, the average crystalline sizes of the AC-AgO and AC-CuO nanocomposite were found to be 5.12 nm and 6.45 nm, respectively.

### 3.3 FE-SEM analysis

Field emission scanning electron microscopy was used to examine the surface morphology of the AC-AgO and AC-CuO nanocomposite, as seen in Figure 3(a and b). The spherical with aggregated morphology, smooth-surfaced morphologies of the as-prepared AC-AgO and Ag-CuOnanocomposite are shown in Figure 3(a,b). In Figure 3(a,b), the carbon is evenly dispersed throughout the CuO, and AgO nanocomposite. The rate of NP nucleation in both pathways was likely affected by high temperatures, which could have been due to product supersaturation and accelerated formation. The NPs' rate of aggregation can reveal information about their shape and structure [16,17].The average particle size of AC-AgO and AC-CuOnanocomposite is approximately 52.32 and 49.25 nm, respectively, and they demonstrate remarkable uniformity, cubic shape, and appropriate separation. Nevertheless, some agglomerates were observed, likely caused by clumping during the washing phase. The results from energy dispersive spectroscopy (EDS) for both AC-AgO and AC-CuO are illustrated in Figure 3. As the analysis only reveals signals for Cu, O, and C,andAg.O,C only presented the EDS results confirmed the formation of AC-AgO and AC-CuO.

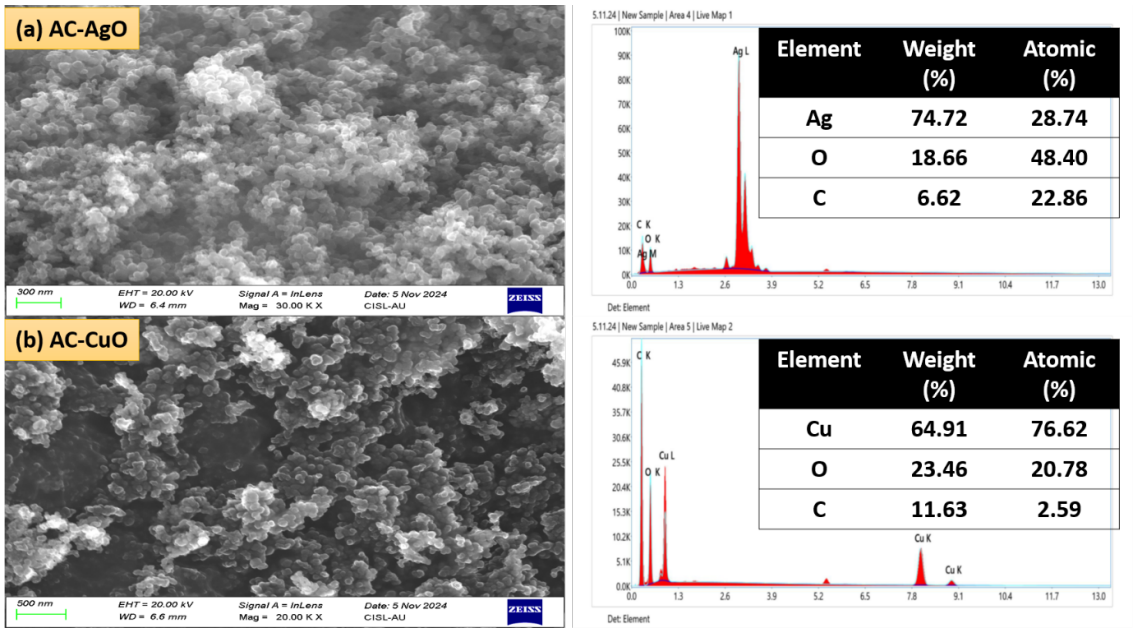


**Figure 3:FE-SEM image of (a) AC-AgO and (b) AC-CuO**

### 3.4 UV-DRS analysis

Using UV-Vis-DRS spectra, the optical characteristics of both AC-AgO and AC-CuO nanocomposite were examined. Figure 4 displays the recorded DRS spectra. The optical reflectance spectra were collected within the wavelength range of 200–800 nm. The well-known Kubelka-Munk equation (3) was used to get the band gap values of AC-AgO and AC-CuO. The calculated band gap energy values for each are 2.68 and 1.98 eV (Figure. 4).

$$\alpha h\nu = A\,(h\nu - E_g)^{1/2} \qquad (3)$$

Where, n = 2 is the direct energy band gap, A is the material constant, and Eg is the bandgap energy [18,19]. The carbon composite in the AC-AgO and AC-CuO material clearly shows how band gap energy is altered when carbon is added, while the band gap of AC-AgO and AC-CuO is decreased. Consequently, it is suggested that the AC-AgO and AC-CuO nanocomposite's lower band gap energy may be used to provide the desired photocatalytic activity.

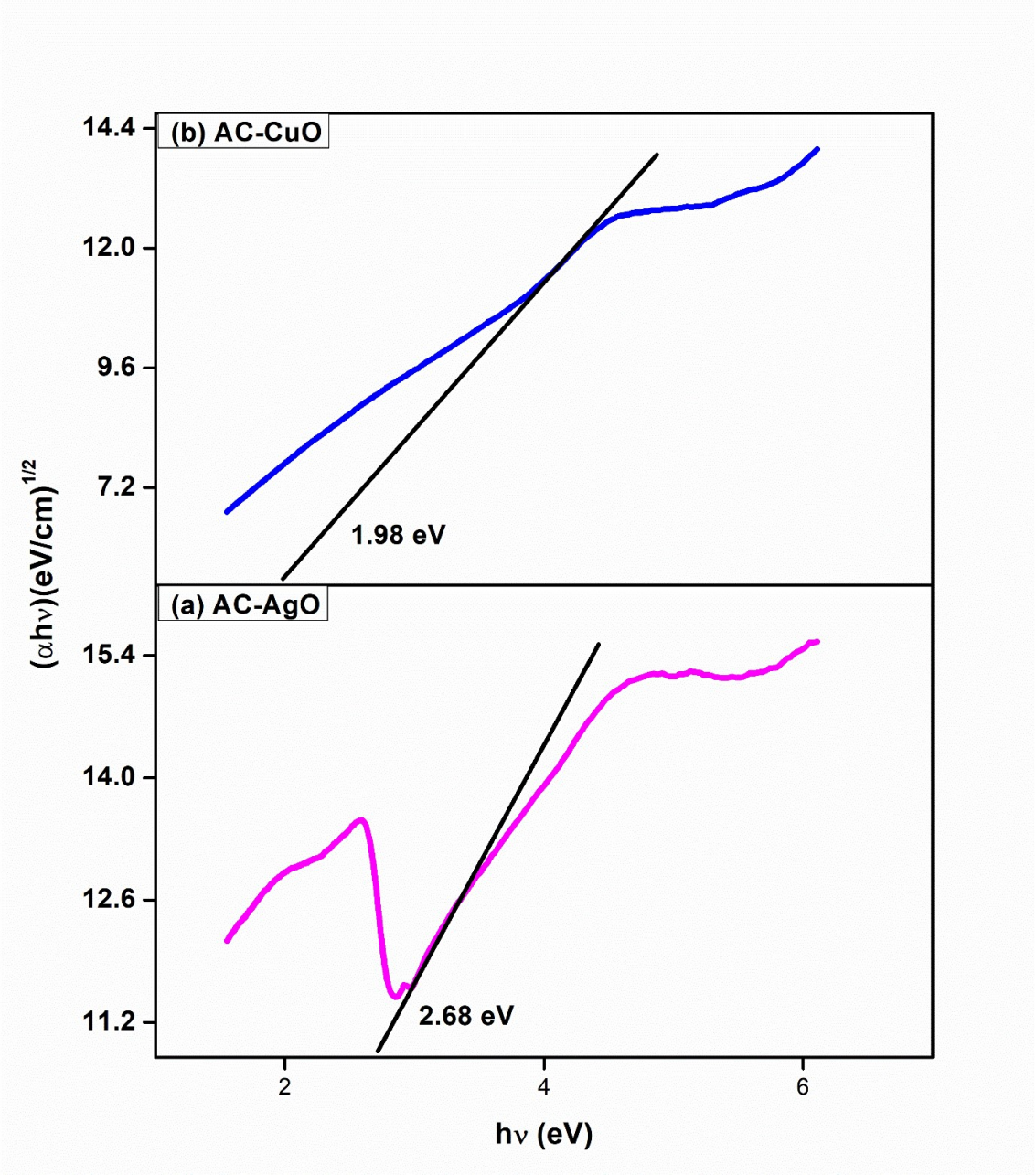


**Figure 4:UV-DRS spectra of (a) AC-AgO and (b) AC-CuO**

### 3.5 Photoluminescence analysis

The Figure 5 illustrates the excitation wavelength effect from the photoluminescence spectra of AC-AgO and AC-AgO. Two emission peaks were seen in the photoluminescence study at 409 nm (blue) and 428 nm (blue) (Figure 5 (a,b). The first one is associated with band-edge emission, whereas the second one results from artifacts. Sharp visible emission peak and a wide UV emission peak, referred to as the near band-edge emission, are present in

the spectrum. The UV emission peaks in Figure 5 are associated with spectra that are situated between 360 and 390 nm. The findings of Figure 5 were obtained using an excitation wavelength of 300 nm. According to the above-calculated Eg, reveals a blue shift with decreasing nanoparticle size as a result of the narrow band gap brought on by an increase in quantum-confinement effects [20,21]. The emission seen at the band edge is ascribed to the recombination of electrons and holes of CuO and AgO-free excitons, a process that is very sensitive to particle size in quantum mechanics. Consequently, the lower intensity of the AC-AgO and AC-CuOnanocomposite indicates that electron and hole recombination is suppressed and that these particles take part in photochemical transformation, thus augmenting the photocatalytic activity of the nanocomposites.

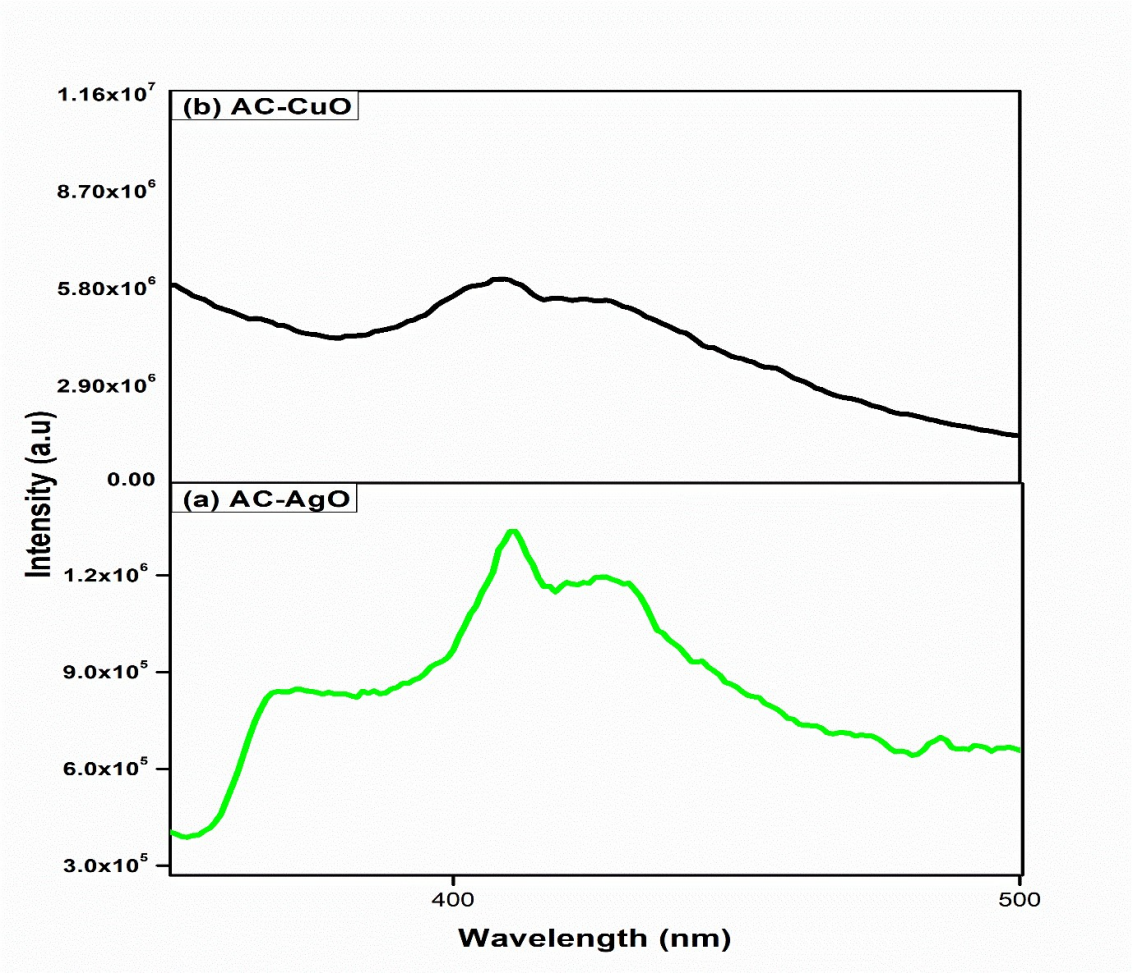


**Figure 5:PL emission spectra of (a) AC-AgO and (b) AC-CuO**

### 3.6 Photocatalytic degradation

The composites' photocatalytic activity is assessed by their ability to remove MB. A 100 mg AC-AgO and AC-CuO nanocomposite was submerged in 100 mL of MB solution and exposed to UV light. 4 mL of the MB solution are taken out of the dye solution every fifteen minutes in order to measure the photocatalytic activity. Figure 6 shows the measurement of MB dye absorption at a wavelength of 665 nm. Equation 1, where $C_0$ is the final dye solution concentration (mg $L^{-1}$) at a specific time period and Ct is the beginning dye solution concentration (mg $L^{-1}$), was used to compute the deterioration rate percentage.

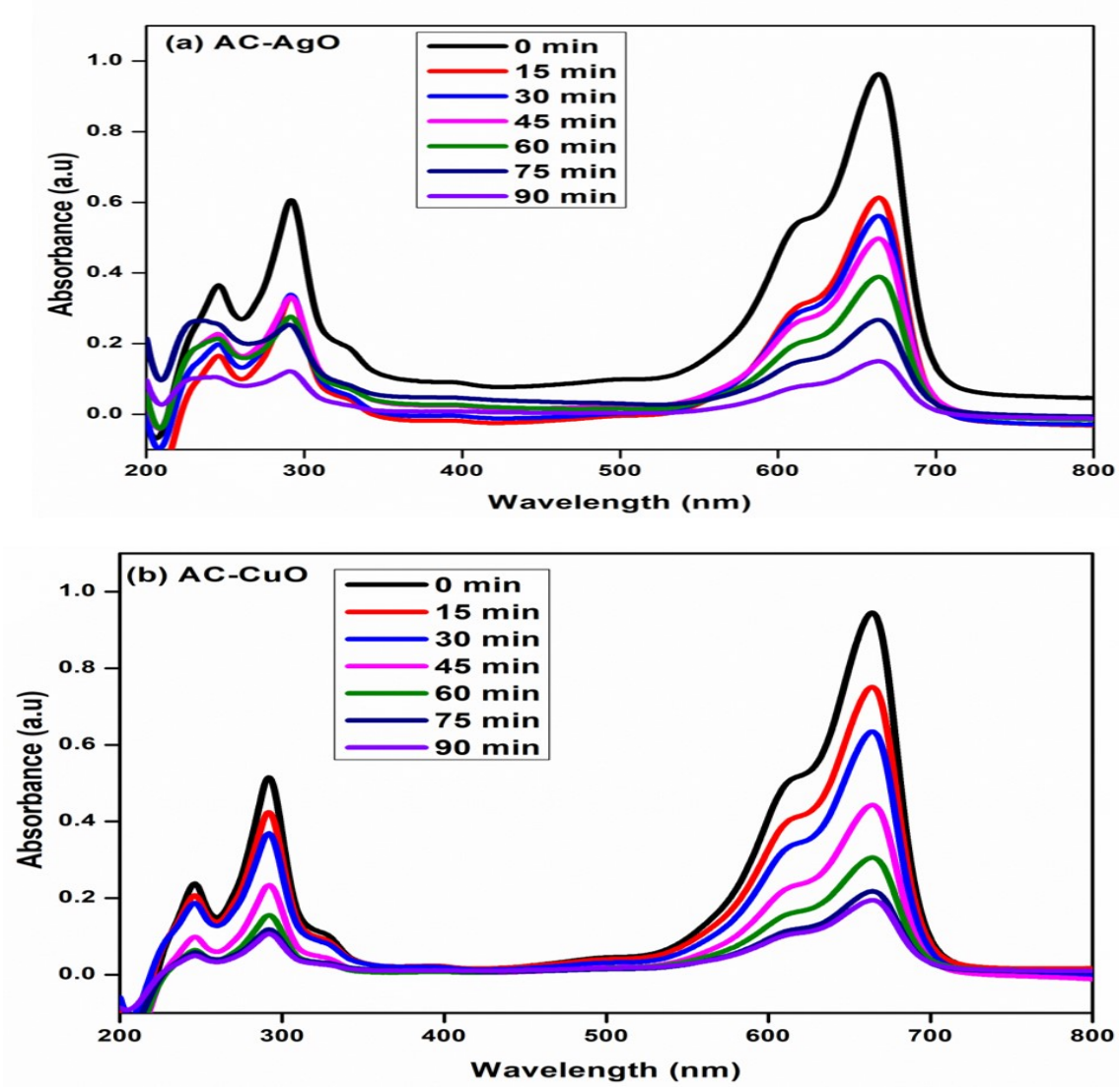


**Figure 6: UV degradation of MB dye (a) AC-AgO and (b) AC-CuO**

Figure 6 (a,b) displays the photocatalytic activity of the produced AC-AgO and AC-CuO nanocomposites. The photocatalytic activity of AC-AgO and AC-CuOnanocomposites is significantly higher. After being exposed to UV radiation for 15 minutes, AC-AgO and AC-CuOnanocomposites totally photodegrade the MB dye. This highlights the need of catalyst in photodegradation. The photocatalytic activity rises with the concentration of Activated Carbon. Figure 6 (a,b) illustrates the MB dye degradation on the catalyst surface during a period of 0 to 90 minutes. The concentration of MB dye falls with increasing time interval .The % degradation efficiency is shown in figure 7.

The formation of hydroxyl radicals on the catalyst surface as a result of electrons moving from the conduction band to the valence band. A hydroxyl radical that is produced have an impact on the dye molecule's conjugation system. Moreover, the holes will react with water to produce radicals called hydroxyls (OH). As has been covered in several literature, superoxide and radicals are the primary cause of the breakdown of dye molecules and the creation of $H_2O$, $CO_2$, and other molecules [22-27].

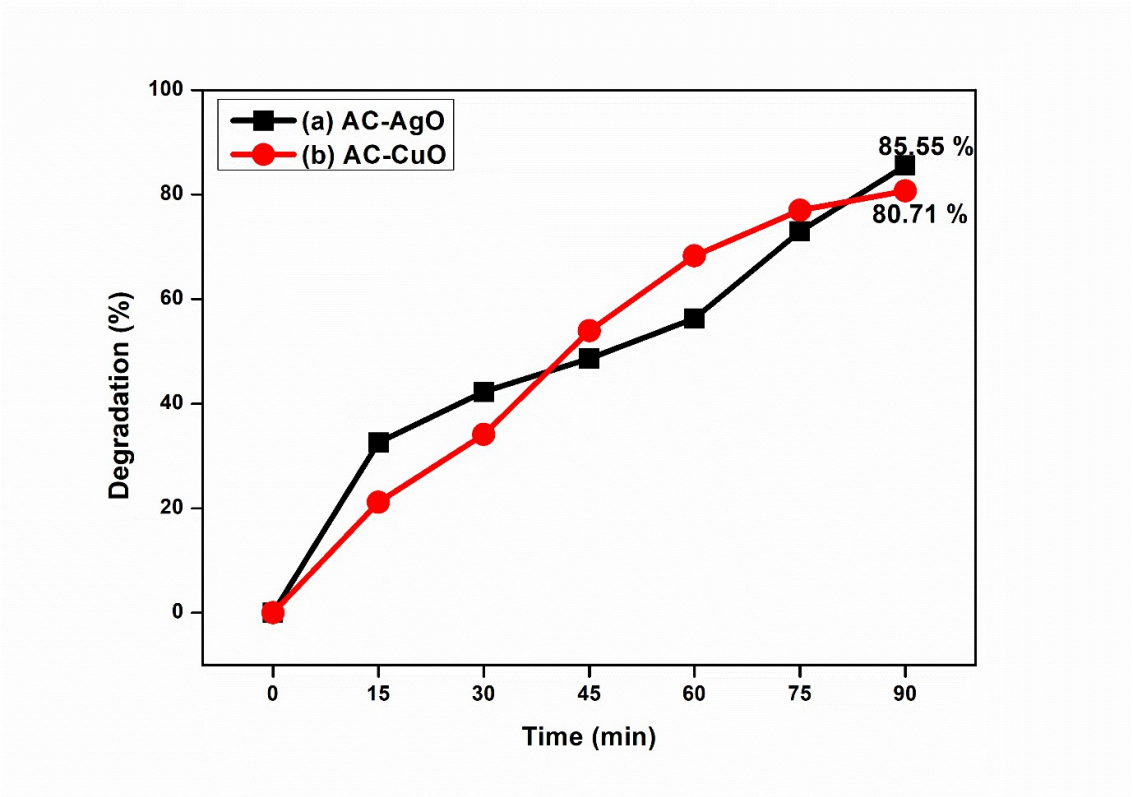


**Figure 7: Dye degradation % of MB dye (a) AC-AgO and (b) AC-CuO**

A photocatalyst is used in the sophisticated oxidation process known as photocatalytic degradation to break down both organic and inorganic contaminants when exposed to light. Because of its effectiveness, minimal energy requirements, and environmentally friendly nature, this approach is frequently employed for environmental cleanup. The experimental techniques, supplies, and methods used to study the photocatalytic degradation process are described in this chapter.

## 4. Conclusion

In this study, AC-AgO and AC-CuO was synthesized using effectively produced. Utilizing FT-IR, XRD, FE-SEM, UV-DRS, and PL, the produced composites were characterized. The chemical bond structure of the composite was determined by the use of FT-IR measurements. The materials used in composites have varying characteristics, according to the XRD study. The FE-SEM results demonstrated the homogenous distribution of the composites. The components of composites have been identified based on the findings of an EDS analysis. MB dye was used to assess the composites photocatalytic activity. MB dye was deteriorated by 85.55% and 80.71 in 90 minutes according to AC-AgO and AC-CuO photocatalytic activity studies, while AC-AgO and AC-CuO demonstrated a higher degradation. Activated Carbon has been shown to improve dye breakdown efficiency of MB dye. The results imply that these could be helpful as potential photocatalysts for the dye pollution photodegradation process.

**Acknowledgement**

None

**Author contribution**

T. Sivasankar contributed in collect primary data, Design the Experiment, do the experimental analysis and overall manuscript writing and finalizing it. B. Karthikeyan was involved in supervision, formal analysis, contribute in draft, check draft, resources and editing manuscript and provided necessary facilities.

**Conflict of interest statement**

The authors declare no conflict of interest in this research work.

**Data availability statement**

Manuscript has no associated data.

## 5. References


1. Abdalameer, N. K., Khalaph, K. A., & Ali, E. M. (2021). Ag/AgO nanoparticles: Green synthesis and investigation of their bacterial inhibition effects. *Materials Today: Proceedings*, *45*, 5788-5792.
2. Anjana, V. N., Joseph, M., Francis, S., Joseph, A., Koshy, E. P., & Mathew, B. (2021). *Microwave assisted green synthesis of silver nanoparticles for optical, catalytic, biological and electrochemical applications. Artif Cells, NanomedicineBiotechnol 49: 438–449*.
3. Chahal, S., Macairan, J. R., Yousefi, N., Tufenkji, N., &Naccache, R. (2021). Green synthesis of carbon dots and their applications. *RSC advances*, *11*(41), 25354-25363.
4. Jiang, Y., Liu, D., Cho, M., Lee, S. S., Zhang, F., Biswas, P., & Fortner, J. D. (2016). In situ photocatalytic synthesis of Ag nanoparticles (nAg) by crumpled graphene oxide composite membranes for filtration and disinfection applications. *Environmental Science & Technology*, *50*(5), 2514-2521.
5. Kulal, D., &Kodialbail, V. S. (2021). Visible light mediated photocatalytic dye degradation using Ag2O/AgO-TiO2 nanocomposite synthesized by extracellular bacterial mediated synthesis-An eco-friendly approach for pollution abatement. *Journal of Environmental Chemical Engineering*, *9*(4), 105389.
6. Iravani, S., Korbekandi, H., Mirmohammadi, S. V., &Zolfaghari, B. (2014). Synthesis of silver nanoparticles: chemical, physical and biological methods. *Research in pharmaceutical sciences*, *9*(6), 385-406.
7. Vijayaram, S., Razafindralambo, H., Sun, Y. Z., Vasantharaj, S., Ghafarifarsani, H., Hoseinifar, S. H., &Raeeszadeh, M. (2024). Applications of green synthesized metal nanoparticles—a review. *Biological Trace Element Research*, *202*(1), 360-386.
8. Said, M. I., & Othman, A. A. (2021). Structural, optical and photocatalytic properties of mesoporousCuO nanoparticles with tunable size and different morphologies. *RSC advances*, *11*(60), 37801-37813.
9. Janoš, P., Buchtová, H., &Rýznarová, M. (2003). Sorption of dyes from aqueous solutions onto fly ash. *Water research*, *37*(20), 4938-4944.
10. Seshadri, S., Bishop, P. L., & Agha, A. M. (1994). Anaerobic/aerobic treatment of selected azo dyes in wastewater. *Waste Management*, *14*(2), 127-137.
11. Hosseinpour-Mashkani SM, Ramezani M. Silver and silver oxide nanoparticles: Synthesis and characterization by thermal decomposition. *Materials Letters*. 2014; 1; 130:259-62.

12. Mohamed, E. A. (2020). Green synthesis of copper & copper oxide nanoparticles using the extract of seedless dates. Heliyon, 6(1).
13. Matei, A., Craciun, G., Romanitan, C., Pachiu, C., &Tucureanu, V. (2023). Biosynthesis and Characterization of Copper Oxide Nanoparticles. *Engineering Proceedings*, *37*(1), 54.
14. Gauri B, Vidya K, Sharada D, Shobha W. Synthesis and characterization of Ag/AgO nanoparticles as alcohol sensor. *Res J Chem Environ*. 2016 ;20(10):1-5.
15. Siddiqui, H., Parra, M. R., Qureshi, M. S., Malik, M. M., &Haque, F. Z. (2018). Studies of structural, optical, and electrical properties associated with defects in sodium-doped copper oxide (CuO/Na) nanostructures. *Journal of materials science*, *53*(12), 8826-8843.
16. Mohammadi M, Hekmatara SH, Moghaddam RS, Darehkordi A. Preparation and optimization photocatalytic activity of polymer-grafted Ag@ AgO core-shell quantum dots. *Environmental Science and Pollution Research*. 2019; 1;26(13):13401-9.
17. Petkova GA, Záruba K, Žvátora P, Král V. Gold and silver nanoparticles for biomolecule immobilization and enzymatic catalysis. *Nanoscale research letters*. 2012; 7:1-0.
18. Mohanaparameswari S, Balachandramohan M, Sasikumar P, Rajeevgandhi C, Vimalan M, Pugazhendhi S, Ganesh Kumar K, Albukhaty S, Sulaiman GM, Abomughaid MM, Abu-Alghayth M. Investigation of structural properties and antibacterial activity of AgO nanoparticle extract from Solanumnigrum/Mentha leaf extracts by green synthesis method. *Green Processing and Synthesis*. 2023; 1;12(1):20230080.
19. Rita A, Sivakumar A, Dhas SS, Dhas SM. Structural, optical and magnetic properties of silver oxide (AgO) nanoparticles at shocked conditions. *Journal of Nanostructure in Chemistry*. 2020; 10:309-16.
20. Shetty V. Solar light active biogenic titanium dioxide embedded silver oxide ($AgO/Ag_2O$@ $TiO_2$) nanocomposite structures for dye degradation by photocatalysis. *Materials Science in Semiconductor Processing*. 2021;1; 132:105923.
21. Balraj B, Arulmozhi M, Siva C, Krithikadevi R. Synthesis, characterization and electrochemical analysis of hydrothermal synthesized AgO incorporated $ZrO_2$ nanostructures. *Journal of Materials Science: Materials in Electronics*. 2017; 28:5906-12.

22. Naveenkumar, R., Karthikeyan, B., &Senthilvelan, S. (2023). Synthesis of bioinspired lotus fiber infused PVA/TiO2 nanocomposites: characterization, thermal, and photocatalytic activity studies. *Biomass Conversion and Biorefinery*, 1-13.
23. Kulal, D., &Kodialbail, V. S. (2021). Visible light mediated photocatalytic dye degradation using Ag2O/AgO-TiO2 nanocomposite synthesized by extracellular bacterial mediated synthesis-An eco-friendly approach for pollution abatement. *Journal of Environmental Chemical Engineering*, *9*(4), 105389.
24. Naveenkumar, R., Karthikeyan, B., &Senthilvelan, S. (2024). Facile Green Synthesis of Activated Biocarbon-Cobalt-Doped TiO2 Nanocomposite for Enhanced Antibacterial Effect and Efficient Photocatalytic for Dye Degradation. *Brazilian Journal of Physics*, *54*(5), 170.
25. Berede, H. T., Andoshe, D. M., Gultom, N. S., Kuo, D. H., Chen, X., Abdullah, H., ...&Zelekew, O. A. (2024). Photocatalytic activity of the biogenic mediated green synthesized CuO nanoparticles confined into MgAl LDH matrix. *Scientific Reports*, *14*(1), 2314.
26. Naveenkumar, R., Karthikeyan, B., &Senthilvelan, S. (2024). Photocatalytic Degradation of Toxic Rhodamine B Dye by Green-Synthesised Activated Carbon-Supported Cobalt Doped ZnO with Further Assessment of ZnO Nanoparticles in Antimicrobial Applications. *ChemistrySelect*, *9*(29), e202401448.
27. Jiang, Y., Liu, D., Cho, M., Lee, S. S., Zhang, F., Biswas, P., & Fortner, J. D. (2016). In situ photocatalytic synthesis of Ag nanoparticles (nAg) by crumpled graphene oxide composite membranes for filtration and disinfection applications. *Environmental Science & Technology*, *50*(5), 2514-2521.